Global Proteomic Analysis of the Chromate Response in Arthrobacter sp Strain FB24

ARTICLE *in* JOURNAL OF PROTEOME RESEARCH · MARCH 2009

Impact Factor: 4.25 · DOI: 10.1021/pr800705f · Source: PubMed

11 AUTHORS, INCLUDING:

Kristene L Henne
Argonne National Laboratory
11 PUBLICATIONS **146** CITATIONS
SEE PROFILE

Gyorgy Babnigg
Argonne National Laboratory
50 PUBLICATIONS **770** CITATIONS
SEE PROFILE

Carol S Giometti
Argonne National Laboratory
110 PUBLICATIONS **2,416** CITATIONS
SEE PROFILE

Dorothea K Thompson
Microbial Insights, Inc.
41 PUBLICATIONS **1,639** CITATIONS
SEE PROFILE

research articles Journal of proteome research

Global Proteomic Analysis of the Chromate Response in *Arthrobacter* sp. Strain FB24

Kristene L. Henne,*,† Joshua E. Turse,§ Carrie D. Nicora,§ Mary S. Lipton,§ Sandra L. Tollaksen,|| Carl Lindberg,|| Gyorgy Babnigg,|| Carol S. Giometti,|| Cindy H. Nakatsu,‡ Dorothea K. Thompson,† and Allan E. Konopka†,§,#

Departments of Biological Sciences and Agronomy, Purdue University, West Lafayette, Indiana 47907, Biological Sciences Division, Pacific Northwest National Laboratory, Richland, Washington 99354, and Biosciences Division, Argonne National Laboratory, Argonne, Illinois 60439

Received September 4, 2008

A global proteomic evaluation of the response of *Arthrobacter* sp. strain FB24 to 5 and 20 mM Cr(VI) was conducted using both two-dimensional gel electrophoresis (2-DGE) and liquid chromatography coupled with tandem mass spectrometry (LC/LC-MS/MS). The changes in protein expression found with 2-DGE indicate alterations in central metabolism and amino acid synthesis. Proteome coverage increased from 22% with 2-DGE to 71% with LC/LC-MS/MS. The proteins exhibiting the highest levels of expression under Cr(VI) stress suggest intracellular sulfur limitation, which could be driven by competition for the sulfate (SO_4^{2-}) transporter by the chromate (CrO_4^{2-}) ion. These results are consistent with the growth defects seen with strain FB24 when Cr(VI) concentrations exceeded 5 mM.

Keywords: *Arthrobacter* • chromium • metal resistance • proteomics • two-dimensional gel electrophoresis • liquid chromatography • mass spectrometry

Introduction

Arthrobacter species are high G + C Gram-positive bacteria that are numerically dominant in both pristine and polluted soils and are known for their ability to survive in extreme environments.[1] *Arthrobacter* was found to be the most common isolate from terrestrial subsurface soils at the Hanford Site in Washington State and from the Savannah River Site in South Carolina. Both were locations of U.S. weapons production facilities and are marked by high-level radioactive waste and accompanying heavy metals such as chromium.[2−5] Chromium is a common contaminant at many waste sites,[6] with trivalent [Cr(III)] and hexavalent [Cr(VI)] forms as the most stable oxidation states. Because of its carcinogenic and mutagenic associations, Cr(VI) is considered to be a serious public health concern.[7] Moreover, Cr(VI) has been shown to inhibit soil microbial activity,[8,9] which can have deleterious effects on soil ecosystem function and sustainability.

Further examination of the metal resistance properties of bacterial isolates from both the Hanford and Savannah River sites demonstrated that *Arthrobacter* species exhibit high levels of resistance to a variety of toxic metals in contrast to other species from the same sites.[2] Despite these findings, very little is known about the genetic or physiological mechanisms driving the success of *Arthrobacter* in metal-contaminated soils. *Arthrobacter* sp. strain FB24 was isolated from soils at a Seymour, IN waste site characterized by high levels of lead and chromium, in addition to the organic pollutants benzene, toluene and xylene.[10] Species strain FB24 was selected for further study based on its high tolerance to a wide variety of toxic heavy metals. Most notably, this strain can survive in the presence of 200 mM potassium chromate.[10] By comparison, most other bacteria [primarily Proteobacteria that enzymatically reduce Cr(VI)] typically only withstand micromolar (μM) concentrations.[11]

Chromate resistance in *Arthrobacter* sp. strain FB24 is speculated to occur primarily through chromate efflux, a process that has only been studied in *Cupriavidus metalliduran*s and *Pseudomonas aeruginosa* to date. These species can tolerate 0.3 and 4 mM chromate, respectively, but the number of genes involved in Cr(VI) resistance in these two strains is different.[12,13] Higher levels of resistance (12−20 mM) have been noted for bacterial isolates from chromium-contaminated soils;[14] however, the genetic determinants of chromate resistance in many of these isolates remain to be determined. Recently, Viti et al. characterized chromate-resistant and chromate-reducing strains of *Pseudomonas* through the use of phenotypic microarrays. The strains that exhibited the highest chromate resistance and reduction potential were found to be more resistant to other toxic ions, protein synthesis inhibitors, and inhibitors of DNA replication.[15] Considering this, it is possible that contributing factors other than dedicated chromate efflux proteins and oxidoreductases have been overlooked in the quest to better understand microbial chromate resistance.

* To whom correspondence should be addressed. Present mailing address: Purdue University, Department of Biological Sciences, 915 West State Street, West Lafayette, IN 47907. Phone: (765) 494-7868. Fax: (765) 494-0876. E-mail: khenne@purdue.edu.

† Department of Biological Sciences, Purdue University.

§ Pacific Northwest National Laboratory.

|| Argonne National Laboratory.

‡ Department of Agronomy, Purdue University.

Present address: Biological Sciences Division, Pacific Northwest National Laboratory, P.O. Box 999, MSIN: P7-50, Richland, WA 99352.

10.1021/pr800705f CCC: $40.75

Published on Web 02/20/2009

The purpose of this study was to examine the global proteomic response of *Arthrobacter* strain FB24 to chromate stress. The FB24 genome has been sequenced by the Department of Energy's Joint Genome Institute (DOE-JGI) and consists of a 4.7 Mb chromosome and three plasmids with sizes of approximately 160, 116, and 96 kb. Of the 4605 genes, 4536 are predicted to encode proteins, 27% of which do not have any function prediction (http://img.jgi.doe.gov). We have employed two-dimensional gel electrophoresis (2-DGE) and liquid chromatography (LC) coupled with tandem mass spectrometry (MS/MS) to determine relative abundance differences in FB24 proteins expressed under different chromate stress conditions. Two-dimensional gel electrophoresis is a well-established and widely accepted method for separation of proteins in complex mixtures.[16,17] When followed by MS identification of proteins of interest, this method offers a convenient avenue for comparing protein profiles of a single strain exposed to various conditions.[16,17] LC-MS/MS provides deeper proteome coverage and, in some cases, greater sensitivity in detecting changes in protein abundance.[18,19] In combination, data from the gel-based and LC-MS/MS approaches resulted in approximately 70% coverage of the predicted proteome, allowing insight into the physiological response of strain FB24 to chromate stress.

Experimental Methods

Bacterial Culture Conditions. *Arthrobacter* sp. strain FB24 was cultivated aerobically at 30 °C in 500-mL batch cultures consisting of either 0.2× (for 2-DGE) or full-strength (for LC-MS/MS) nutrient broth (Difco, Sparks, MD) amended with 0, 5, or 20 mM potassium chromate [K_2CrO_4, (Sigma-Aldrich, St. Louis, MO)]. Log-phase cells were harvested from 3 cultures per growth condition by centrifugation and washed twice in 1 mM Tris buffer (pH 7.5). Stationary-phase cells were harvested from a separate, untreated control culture for inclusion in the LC-MS/MS study. Cell pellets were stored at −80 °C until processed.

Sample Preparation for 2-DGE. Whole-cell lysates were prepared for 2-DGE analysis by resuspending cell pellets in solubilization buffer [9 M urea, 4% NP-40, 2% ampholytes (pH 3−10, Bio-Rad, Hercules, CA), 2% β-mercaptoethanol and protease inhibitors (complete mini protease inhibitor cocktail, Roche, Indianapolis, IN)]. The cell suspension was sonicated on ice for 8 min in 30 s pulses using a Virsonic100 cell disruptor (VirTis, Gardiner, NY) with an output of 10−14 W. Unbroken cells and cell debris were removed by low-speed centrifugation and protein extracts were centrifuged at 200 000*g* for 30 min in a Beckman TLA-100 ultracentrifuge to remove nucleic acids. The final supernatant was collected as the whole cell extract (WCE). Protein extracts were concentrated using the ReadyPrep 2D Cleanup Kit (Bio-Rad, Hercules, CA) and resuspended in solubilization buffer. Protein concentration was determined using a modification of the Bradford protein assay.[20]

Two-Dimensional Gel Electrophoresis. For analytical 2-DGE, 40 μg of protein sample was separated in the first dimension by isoelectric focusing (IEF) for 14 000 Vh in tube gels containing a mixture of four parts pH 5−7 and one part pH 3−10 carrier ampholytes (Bio-Rad, Hercules, CA). The IEF gels were then equilibrated in SDS reducing buffer containing 5% DTT. Proteins were separated in the second dimension by SDS-PAGE in a 10−17% acrylamide gradient.[21−23] A set of 2-DGE standards consisting of β-galactosidase, bovine serum albumin, actin, carbonic anhydrase and trypsin inhibitor was included with each gel set for molecular weight (MW) and isoelectric point (p*I*) calibration. Proteins were visualized by silver staining.[24] For preparative 2-DGE, 150 μg of protein samples was separated in the same manner; however, proteins were visualized by Coomassie staining.[25]

2-DGE Data Acquisition and Image Analysis. To detect significant differences in protein abundance between growth conditions [5 and 20 mM Cr(VI) gels were compared to the no chromate reference gels], silver-stained gel images were digitized using an Eikonix1412 scanner interfaced with a VAX 4000−90 workstation. The images were transferred to a PC, converted to TIFF format and processed for spot detection and pattern matching using the Progenesis software (Version 2003.03; Nonlinear USA, Research Triangle Park, NC). Each growth condition was represented by three experimental replicates (derived from three independent batch cultures) and one of three replicate 2-DGE patterns for each experimental replicate resulting in a total of three gels *per* growth condition used in the analysis. A representative 2-DGE image of proteins from lysates of cells grown without Cr(VI) was used as the reference pattern. All 2-DGE patterns were matched to the reference pattern using the Progenesis default spot detection parameters together with the combined warping and matching option to assign corresponding identification numbers to matched spots in each pattern. Normalization of spot intensities was carried out as described previously.[26] The resulting data were exported to Excel and filtered according to the following criteria: total spot intensity of 10 000 or greater; spot relative abundance less than 0.6 or greater than 2 [Cr(VI) versus no Cr(VI) control]; coefficient of variation across samples less than 25; Student's *t* test *p*-value less than 0.05.

Peptide Mass Spectrometry for Protein Identification. Protein spots showing significant ($p < 0.05$) differences in abundance between growth conditions were identified by peptide mass analysis. All protein spots were first excised from 4−7 silver-stained gels that were used for comparative analyses and submitted for LC-MS/MS identification at Argonne National Laboratory. To validate identifications and, in cases where initial Mascot scores were poor, peptide mass analysis was also done using Coomassie Brilliant Blue (CBB)-stained spots from 2D- electrophoresis gels generated using 150 μg of total protein. Replicate gels containing 40 μg of total protein per gel were included in the same electrophoresis run and silver stained. The resulting CBB and silver-stained protein patterns were similar, so that CBB-stained gels could be overlaid onto silver-stained gels and matching spots and spot constellations (surrounding spots as landmarks) could be used to guide the protein spot excision process. Identification of protein spots was verified by independent analysis at the W.M. Keck Foundation Biotechnology Resource Laboratory, Yale University, New Haven, CT. Protein spots were destained, dehydrated and reduced with Tris (2-carboxyethyl) phosphine (TCEP; Pierce), alkylated with iodoacetamide, and digested with trypsin (Promega [Madison, WI] sequence grade trypsin, 12.5 ng/μL). The resulting peptides were eluted from the gel pieces by extracting three times, first with equal parts of 25 mM ammonium bicarbonate and acetonitrile, then twice with equal parts of 5% (v/v) formic acid and acetonitrile.

Tryptic peptide analysis at Argonne National Laboratory was conducted as described previously.[26] The MS/MS spectra were used in Mascot searches of the predicted protein sequence of the *Arthrobacter* sp. FB24 ORF database using the total genome sequence provided by the Department of Energy-Joint Genome

Initiative (ftp://ftp.jgi-psf.org/pub/JGI_data/Microbial/arthrobacter_fb24/Finished2006/3634492.finished.fsa). Ion scores were determined by $-10 \times \mathrm{Log}(p)$, where p is the probability that the observed match was a random event; individual ion scores greater than 50 indicate identity or extensive homology ($p < 0.05$). Protein scores are derived from ion scores as a non-probabilistic basis for ranking protein hits.[27] Protein identifications reported using the Mascot search algorithm had scores greater than 100 with at least two peptides matching the theoretical masses of tryptic peptides.

Preparation of *Arthrobacter* Digests for LC-MS/MS. Preparation of *Arthrobacter* digests and LC-MS/MS analysis was performed by the Environmental Molecular Sciences Laboratory (EMSL) at Pacific Northwest National Laboratory (PNNL), Richland, WA. Samples were prepared from cell lysate as described previously.[27,28] In addition to a global preparation, the sample was partitioned into soluble and insoluble partitions. Sample supernatant was used for the soluble preparation, while the pellet was used for the insoluble preparation.

Strong Cation Exchange (SCX) Fractionation and Capillary LC-MS/MS Analysis. Trypsin-digested *Arthrobacter* samples from the various growth conditions were fractionated into 25 fractions using gradient strong cation exchange chromatography, as described previously.[29] Fractions were concentrated to about 1 μg/μL and analyzed by LC-MS/MS using an LTQ spectrometer (ThermoFinnigan, San Jose, CA), operated in a data-dependent mode, over segmented m/z ranges. The MS/MS spectra were analyzed using SEQUEST[30] against a database of theoretical masses generated from the *Arthrobacter* FastA. Fully and partially tryptic peptides identified by SEQUEST were used to generate the data for quantitation. Each SCX fraction was analyzed with an automated custom-built capillary HPLC system coupled online with an LTQ ion trap mass spectrometer (ThermoElectron, San Jose, CA) using an electrospray ionization interface. The reversed phase capillary column was prepared by slurry packing 3-m Jupiter C18 particles (Phenomenex, Torrence, CA) into a 150 μm i.d. (internal diameter) $\times$ 65 cm fused silica capillary (Polymicro Technologies, Phoenix, AZ). The mobile phase solvents consisted of (A) 0.2% acetic acid and 0.05% TFA in water and (B) 0.1% TFA in 90% acetonitrile. An exponential gradient was used for the separation, which started with 100% A and gradually increased to 60% B over 100 min. The instrument was operated in a data-dependent mode with an m/z range of 400−2000. The five most abundant ions from each MS scan were selected for further MS/MS analysis using a normalized collision energy setting of 35%. Dynamic exclusion was applied to avoid repeating analyses of the same abundant precursor ion.

LC-MS/MS Data Analysis. The SEQUEST algorithm[30] (ThermoElectron) was used to search the LC-MS/MS data against the database of theoretical masses generated from the *Arthrobacter* sp. strain FB24 FastA available from the DOE-JGI (available online at http://tinyurl.com/2zfpuw) and a sequence-reversed database. The following criteria were used to filter raw SEQUEST results: (1) Xcorr 1.9 for charge state +1 full tryptic peptides; (2) Xcorr 2.2 for charge state +2 full and partial tryptic peptides; and (3) Xcorr 3.75 for charge state +3 full tryptic and partial tryptic peptides. The delta correlation value (DelCN2) > 0.1 was used in all cases.[31] These criteria were established based on probability-based evaluation using sequence-reversed database searching as previously described to provide >95% overall confidence level for the entire set of unique peptide identifications (<5% false positive rate).[32]The identified proteins were categorized based on their cellular locations and biological processes according to Gene Ontology (GO) information obtained from the European Bioinformatics Institute (http://tinyurl.com/2ckfsd) as well as by the Clusters of Orthologous Groups (COG) function categories available in The Integrated Microbial Genomes (IMG) system (http://tinyurl.com/27eyv3).

Protein Expression Analysis Using GeneSpring. Raw data from SEQUEST were imported to Microsoft Access, where they were filtered to remove peptides with more than one parent protein as well as peptides that were not observed at least twice. Expression analysis was carried out using Agilent GeneSpring GX v 7.3.1. Data were analyzed using the 0 mM chromate/log phase growth condition as the basal state. MS/MS spectral count information for the identified proteins was used to provide a measure of relative protein abundances.[33−35] Fold change in protein abundance was derived by comparing relative protein abundances from bacteria in log-phase growth, with no chromate stress to either chromate stress conditions or stationary-phase growth in the absence of chromate. All values reported reflect the fold difference between the control state and the experimental state. Clustering was performed using average linkage and Pearson correlation.

Results and Discussion

2-DGE Reveals Differentially Expressed Proteins Under Chromate Stress. *Arthrobacter* sp. strain FB24 grows at near-normal rates and yields up to chromate concentrations of 5 mM. At 5 mM (and up to 200 mM) chromate, strain FB24 exhibits reductions in growth rate and biomass yield. In particular, growth rate decreases by 29 and 42% at 5 and 20 mM Cr(VI), respectively, and the biomass yields decrease by 55 and 63%, respectively, compared to 0 mM Cr(VI) control cultures (Growth curve and culture conditions provided in Supplementary Figure 1 in Supporting Information). We were interested in interrogating the cellular proteomic response to these Cr(VI)-induced growth defects. A total of 1000 different protein spots were detected by 2-DGE from FB24 cells grown in 0, 5, and 20 mM Cr(VI), representing 22% of the potential 4536 protein-coding ORFs within the genome. Twenty-six proteins exhibited significant ($p < 0.05$) differences in abundance in either 5 or 20 mM Cr(VI) relative to those found in the absence of chromate (Figure 1). Exposure to 5 mM Cr(VI) resulted in the increased abundance of 5 proteins and decreased abundance of 6 proteins, whereas exposure to 20 mM Cr(VI) resulted in the increased abundance of 9 proteins and the decreased abundance of 11 proteins. Five proteins showed similar abundance trends under both chromate conditions. Nineteen of these proteins were identified with Mascot scores of 100 or greater with at least 2 MS/MS spectra matching the same protein entry in the database searched (Table 1).

Most of the proteins with altered expression function in central carbon and amino acid biosynthesis, which is consistent with the growth defects exhibited by strain FB24 in 5 and 20 mM Cr(VI). Glycolytic enzymes and enzymes involved in energy production may be subject to inactivation via oxidation and expression may also be affected by the thiol/disulfide balance.[36,37] For instance, phosphoenolpyruvate carboxykinase, the pyruvate dehydrogenase complex, malate dehydrogenase and glyceraldehyde-3-phosphate dehydrogenase have all exhibited oxidation-mediated inactivation in various systems.[38−40] Each of these proteins demonstrated a decrease in abundance in the Cr(VI)-treated samples. Conversely, transketolase exhibited a 2.4-fold increase in abundance in 20 mM Cr(VI). Transketolase,

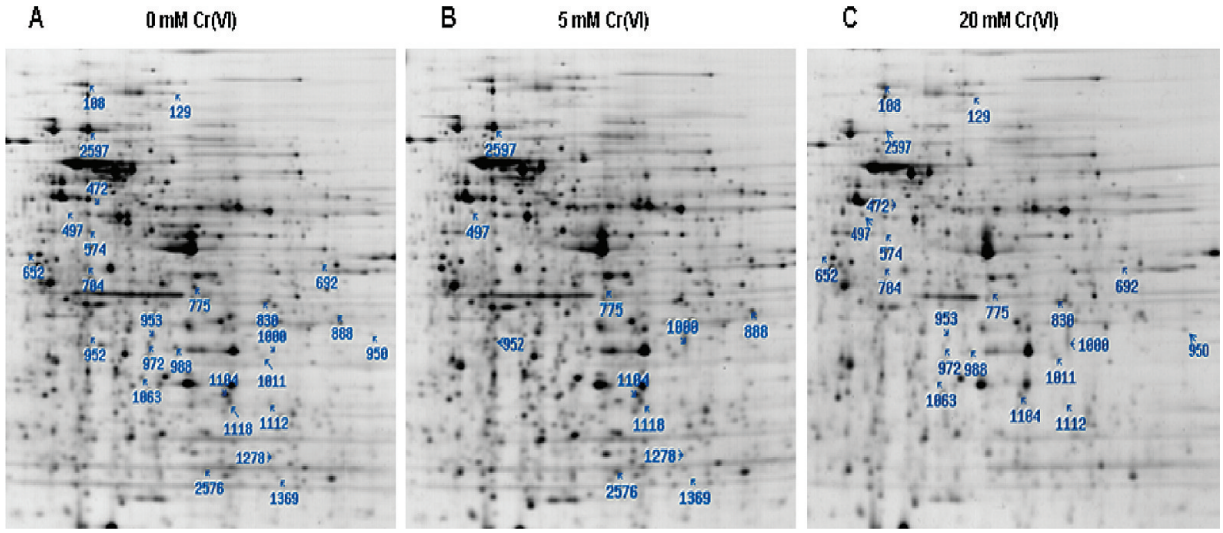

Figure 1. 2-DGE profiles of *Arthrobacter* sp. strain FB24 proteins in response to 5 mM Cr(VI). (A) 0 mM Cr(VI) control; (B) 5 mM Cr(VI); (C) 20 mM Cr(VI). Proteins showing significant ($p < 0.05$) changes in abundance are marked in blue. Panel A depicts all of the protein spots with significant changes in abundance, whereas panels B and C depict protein spots with significant changes in 5 and 20 mM Cr(VI), respectively. Gels were loaded with 40 μg of total protein and spots were visualized with silver staining.

Table 1. Protein Identifications from 2-DGE Analysis

gel spot number	locus	relative abundance Cr(VI)/no Cr(VI)	Students *t* test (*p*-value)	Mascot score	protein identification
			Proteins Differentially Expressed under 5 mM Cr(VI)		
888	3942	3.0	0.0003	673	Aldo/keto reductase
952	1058	2.3	0.0035	172	Oxidoreductase
1278	4418	0.53	0.0047	692	Iron (metal) dependent repressor, DtxR family
1369	3395	0.42	0.028	759	Transcriptional regulator, Crp/Fnr family
2576	0093	2.1	0.016	689	LamB/YcsF family protein
			Proteins Differentially Expressed under 20 mM Cr(VI)		
108	1434	2.0	0.0021	2667	Polyribonucleotide nucleotidyltransferase
129	2097	2.4	0.0071	1222	Transketolase
472	3062	3.3	0.0006	3113	Cystathionine beta-synthase
574	2096	0.60	0.0151	687	Transaldolase
652	3994	0.44	0.0032	735	Malate dehydrogenase (oxaloacetate-decarboxylating)
692	1499	2.2	0.0035	384	Acetylornithine/succinylornithine aminotransferases
704	0607	0.61	0.0081	1189	Extracellular solute-binding protein, family 1
830	1414	2.3	0.0026	621	NusA antitermination factor
950	1649	2.3	0.0070	78	Aldo-keto reductase
988	2087	0.49	0.0015	179	Glyceraldehyde-3-phosphate dehydrogenase, type 1
1011	2189	2.1	0.0003	516	Band 7 protein
			Proteins Differentially Expressed under Both Conditions[a]		
497	2248	3.7	0.0001	862	Glycerol kinase
		3.4	0.0004		
775	3192	0.58	0.0018	948	Pyruvate dehydrogenase complex subunit
		0.55	0.0034		
1104	0627	0.44	0.0012	848	Nuclear export factor, GLE 1
		0.42	0.0005		
2597	0667	0.60	0.0011	1195	Phosphoenolpyruvate carboxykinase (GTP)
		0.18	0.0107		

[a] Top numbers for relative abundance and Students *t* test are for the 5 mM Cr(VI) analysis. Bottom numbers are for the 20 mM Cr(VI) analysis.

together with transaldolase, provides a link between the glycolytic and pentose phosphate pathways. Disrupting flux through these two pathways could affect the production of growth precursors and cellular redox balance, which, in turn, may inhibit growth.[41]

As a structural analogue of sulfate, chromate has been shown to competitively inhibit sulfate transport,[12,42] which may lead to a depletion of sulfur-containing amino acids within the cell. Increasing the flux through pathways producing such amino acids as cysteine may help to overcome this depletion. We detected a 3-fold increase in cystathionine beta-synthase (Arth_3062) when FB24 was grown at 20 mM Cr(VI). Up-regulation of genes involved in cysteine synthesis has been noted in other chromate-stressed bacteria.[43,44] Cysteine synthesis is important not only for biosynthesis, but also for oxidative stress responses by conserving the thiol/disulfide balance within the cell. Central metabolic pathways have been shown to be affected by alterations in this balance, so steps taken to replenish thiol pools can ultimately impact the cellular metabolic potential.[36,37]

Table 2. Correlation of Peptide Count Data for Proteins in Each Experimental Condition Compared to the 0 mM Cr(VI) Log Phase Control Condition[a]

sample comparisons	Pearson correlation coefficient, *r*	95% confidence interval	*r*-squared	number of XY pairs
		Global Partition		
0 Cr(VI) vs 5 mM Cr(VI)	0.96	0.95 to 0.96	0.92	2771
0 Cr(VI) vs 20 mM Cr(VI)	0.93	0.93 to 0.94	0.87	2176
5 Cr(VI) vs 20 mM Cr(VI)	0.95	0.95 to 0.95	0.90	2092
		Soluble Partition		
0 Cr(VI) vs 5 mM Cr(VI)	0.96	0.95 to 0.96	0.91	2100
0 Cr(VI) vs 20 mM Cr(VI)	0.93	0.92 to 0.93	0.86	2083
5 Cr(VI) vs 20 mM Cr(VI)	0.96	0.95 to 0.96	0.91	1961
		Insoluble Partition		
0 Cr(VI) vs 5 mM Cr(VI)	0.90	0.89 to 0.91	0.81	1823
0 Cr(VI) vs 20 mM Cr(VI)	0.89	0.88 to 0.90	0.79	1728
5 Cr(VI) vs 20 mM Cr(VI)	0.89	0.88 to 0.90	0.79	1625

[a] Decrease in correlation as Cr(VI) concentration increased reflects differential expression of proteins in response to 5 and 20 mM Cr(VI). Correlations were generated using GraphPad Prism from raw peptide count data for all proteins in all conditions derived from GeneSpring GX v 7.3.

Unlike FB24, where most of the proteins identified from 2-DGE are involved in central carbon metabolism and amino acid biosynthesis, other bacteria exhibited more of a general and oxidative stress response. Two-dimensional gel electrophoretic analysis of *Escherichia coli* exposed to 0.25 mM Cr(VI) showed increased abundance in cysteine synthase and sulfate adenylyltransferase.[43] That study further revealed high expression of superoxide dismutase, the stringent response protein, SspA and stress-responsive outer membrane proteins (OmpA, OmpW). Analysis of the transcriptome of *Caulobacter crescentus* in response to 0.05 mM Cr(VI) yielded results similar to that of the 2-DGE study in *E. coli*, where the majority of genes upregulated in response to chromate had functions related to oxidative, starvation and membrane stress.[45] The 2-DGE data for FB24 under 5 and 20 mM Cr(VI) point to overall metabolic changes rather than oxidative or general stress responses as were seen in *E. coli* and *C. crescentus*. An inference from this observation is that constitutive and induced resistance mechanisms to Cr(VI) in FB24 are adequate to prevent the induction of stress responses, and that reductions in growth rate and yield upon exposure to Cr(VI) might be due to other specific metabolic changes. Transcriptomic and proteomic studies with *Shewanella oneidensis* MR-1 exposed to Cr(VI) revealed upregulation of the sulfate uptake system, in addition to general and oxidative stress responses.[44,46] As Proteobacteria, these three species are structurally and physiologically different than FB24, an Actinobacterium. These differences, in addition to the higher Cr(VI) resistance of FB24, (*E. coli* and *C. crescentus* showed growth inhibition in the presence of 0.25 and 0.05 mM Cr, respectively;[43,45] the lethal dose for *S. oneidensis* MR-1 is 2 mM[46]) likely contribute to the distinct responses to chromate among the strains.

Global Detection of Proteins Using LC/LC-MS/MS Based Proteomics. To obtain a more comprehensive inventory of proteins from *Arthrobacter* sp. strain FB24 grown under different conditions of chromate stress, global proteomic profiles of strain FB24 from different growth states were determined using LC/LC-MS/MS. Two-dimensional gel electrophoresis is useful for the analysis of soluble and mildly hydrophobic proteins, but is constrained by isoelectric point and molecular weight boundaries and may not be adequate for membrane-associated proteins. Gel-free based approaches, as used here, overcome these limitations by reducing sample complexity and alleviating solubility issues by using digested proteins (peptides)

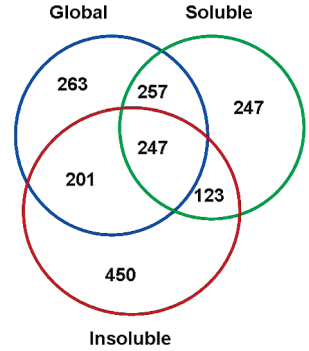

Figure 2. Venn diagram showing overlap of proteins from the global, soluble and insoluble partitions. The values shown are the number of proteins exhibiting a 2-fold difference in abundance in either 5 or 20 mM Cr(VI) log-phase and 0 mM Cr(VI) stationary-phase cultures compared to 0 mM Cr(VI) log-phase control cultures.

as the sample material.[47] Protein expression profiles were examined from midlogarithmic phase cultures of FB24 grown in the presence of 0, 5, and 20 mM chromate, in addition to stationary-phase cells grown without chromate. Correlation of peptide abundance per protein was lower in cells exposed to 20 mM Cr(VI) than in cells exposed to 5 mM Cr(VI) when compared to the no chromate log-phase condition, indicating a greater degree of differential protein expression as the exposure level increased. The correlation coefficients further reveal that FB24 elicits differential protein expression between the 5 and 20 mM Cr(VI) conditions (Table 2).

Proteins were identified from 619 942 measurements of 56 920 high quality peptides. A total of 3220 proteins were observed in the entire data set, corresponding to 71% of the potential 4536 protein-coding ORFs within the genome. Of the proteins observed, 968 in the global partition, 874 in the soluble partition and 1021 in the insoluble partition exhibited a 2-fold difference in comparison to the reference state (cells undergoing exponential growth in the absence of chromate). The Venn diagram (Figure 2) illustrates the overlap between partitions. A total of 247 proteins exhibiting a 2-fold difference were observed in all partitions; however, the fold difference in each partition is not necessarily the same (see Supplementary Tables 1−3 in Supporting Information).

Most proteins with altered abundance fell within COG categories associated with transcription (8−11%), amino acid

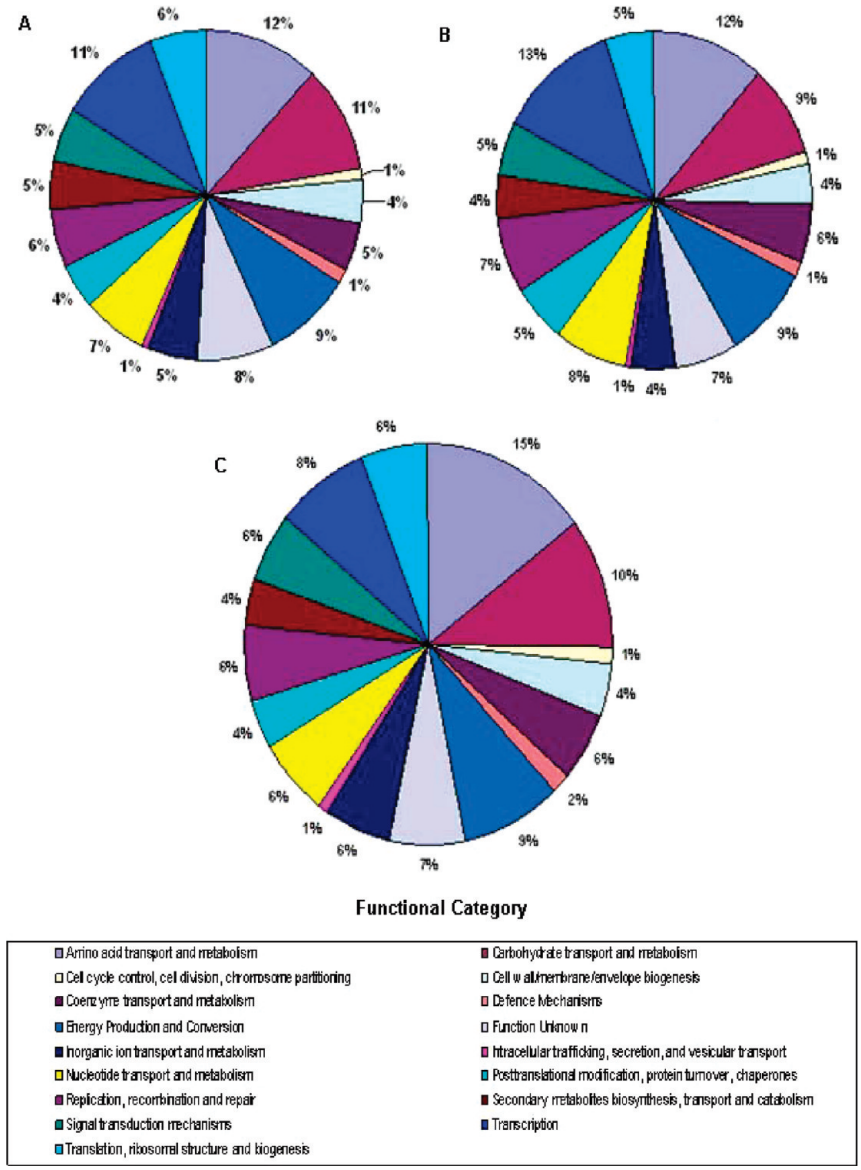

Figure 3. Grouping of differentially expressed proteins according to COG functional categories in the global (A), soluble (B) and insoluble (C) partitions. The group "General Function Prediction Only" was removed due to overlap of proteins with other categories.

transport and metabolism (12−15%), energy production and conversion (9%), and carbohydrate transport and metabolism (9−11%). The percentage of proteins in each of the COG categories followed similar trends across cellular partitions (Figure 3). The predominance of proteins with metabolic or energy functions that exhibit altered expression during growth on chromate are consistent with the observed reductions in growth rate and yield. Further data mining and annotation advances could reveal additional insights, as 20% or more of the differentially expressed proteins were either assigned no COG role or to the category of Function Unknown.

Proteins with Increased Abundance in Chromate. To identify proteins with increased abundance in the Cr(VI) conditions and across all three partitions, the data were clustered according to relative protein abundance to generate a global heat map (Figure 4). Four sections of the heat map which consist of 78, 47, 43, and 39 proteins, respectively, were chosen for further analysis based on increased expression in each Cr(VI) condition and across the cellular partitions. The subsections of the global heat map contain several proteins with highly increased abundance compared to the no Cr(VI) controls. Selected proteins and the corresponding ORF number and abundance changes are provided in Table 3. The major functional categories comprised by this subset of proteins, as discussed below, include DNA recombination, replication and repair, and proteins potentially involved in the uptake of alternative sulfur sources.

Proteins with Protective Functions. Twelve proteins involved in DNA replication, recombination and repair showed greater than a 2-fold increase in abundance under chromate stress in relation to the no chromate, log-phase growth condition. The highest changes were noted for UvrD/REP helicase domain proteins (Arth_2756 and Arth_2757), which exhibited approximately a 20-fold increase in abundance at both 5 and 20 mM Cr(VI) in the insoluble fraction. Two other stress-responsive proteins, Arth_0334 and Arth_0761, exhibited increased abundance in the presence of Cr(VI) in the global and soluble partitions. Both of these proteins are described as Ferritin, Dps family proteins, which function in the sequestration of iron and the protection of DNA under oxidative stress.[48]

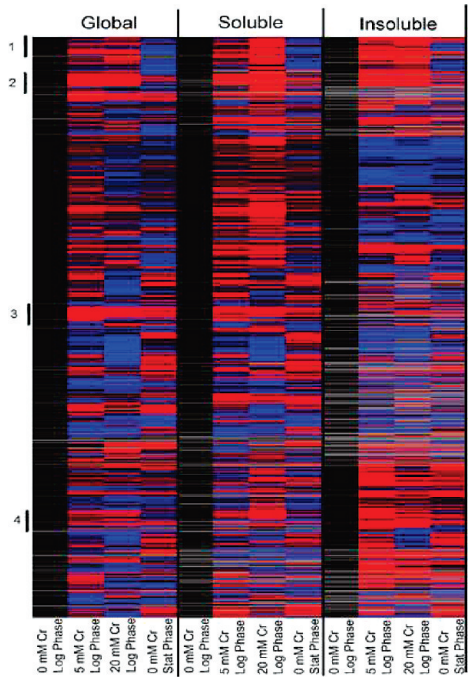

Figure 4. Heat map showing expression of all proteins detected by LC/LC-MS/MS. Peptide count data for each experimental condition were compared to the values for the 0 mM Cr(VI) control condition. Fold-differences were normalized using the values for the 0 mM Cr(VI) condition (black columns). Colors shown indicate the following: red, increased abundance; blue, decreased abundance; black, no change; and gray, no data. Sections 1−4 represent clusters showing increased abundance in each Cr(VI) condition for at least 2 partitions that were selected for further analysis.

The increased abundance of proteins involved in DNA protection, such as the helicase domain proteins and Ferritin, Dps family proteins, suggests that they may play an important role in alleviating chromate stress in strain FB24. A similar protective role was indicated in *P. aeruginosa*, where the inactivation of DNA helicase genes resulted in increased sensitivity to chromate.[49] The up-regulation of genes involved in iron storage and transport was also observed in a recent study of *S. oneidensis* MR-1 undergoing acute chromate challenge.[44] Likewise, defects within the iron transport system in *E. coli* led to sensitivity to Cr(III), the effects of which were reversed by the addition of excess iron to the growth medium.[50] The results from these two studies suggest a link between chromium toxicity and iron uptake and metabolism. Ferrous iron [Fe(II)] can directly participate in Cr(VI) reduction and the formation of reactive transient intermediates, Cr(V) and Cr(IV). In turn, Fenton-type reactions catalyzed by Cr(V) can produce hydroxyl radicals, further enhancing chromium-induced toxicity.[51] It is probable that the iron sequestration properties of Dps and ferritin proteins protect cellular macromolecules against oxidative damage resulting from this type of redox cycling.

Proteins with Putative Functions in the Sulfur Limitation Response. A number of proteins potentially involved in reversing the effects of cellular sulfur limitation exhibited increased abundance under Cr(VI) stress. Several protein clusters suspected to be involved in sulfate uptake and metabolism (Arth_0857−0858 and Arth_3122−3125), the uptake of alternative sulfur sources (Arth_3115−3117) and cysteine synthesis (Arth_2446−2447 and Arth_3122−3125) had fold-differences ranging from 2- to 108-fold in 5 or 20 mM Cr(VI) compared to the no-Cr(VI) control (Table 3). The increased abundance of this group of proteins is suggestive of chromate-induced sulfur limitation in FB24. Further experimentation such as supplementing Cr(VI)-exposed cells with various sulfur sources to determine if the growth defects or the expression profiles of the proteins involved in the sulfur-limitation response are reversed would be beneficial in providing direct evidence to support this conclusion. However, certain conjectures can be made based on the expression of analogous proteins in other organisms under conditions of either sulfur limitation or Cr(VI) stress.

Arth_3115−3117 all contain conserved domains that point to the uptake of aliphatic sulfonates, which is likely to occur when sulfate is in short supply, as may occur during competition of chromate for the sulfate uptake transporter.[12,42] Studies in *E. coli* and *Bacillus subtilis* revealed that the expression of gene clusters encoding alkanesulfonate transporters is increased under conditions of sulfate and cysteine deprivation for the utilization of other sulfur sources such as taurine.[52,53] Arth_3905, a class C flavoprotein monooxygenase with a conserved nitrilotriacetate monooxygenase domain, is one of the most abundant proteins in this study, exhibiting a 108-fold increase in 5 mM Cr(VI) and 58-fold increase in 20 mM Cr(VI) for the global partition. A two-sequence alignment revealed that this protein shares 24% amino acid identity and 40% similarity to SsuD, the *E. coli* alkanesulfonate monooxygenase (gi accession number 2507139). SsuD also exhibited increased protein abundance in response to Cr(VI) in *E. coli*,[43] and acute Cr(VI) exposure in *S. oneidensis* MR-1 led to the increased abundance of proteins that are involved in the sulfate transport system.[44] Both *E. coli* and *B. subtilis* utilize alkanesulfonate monooxygenase to produce sulfites from sulfonates; sulfite can then be used as a sulfur source by the cell. In *E. coli*, the monooxygenase is located in the same gene cluster as the sulfonate transporters, whereas in *B. subtilis*, it is predicted to lie somewhere else on the chromosome.[52,53] Given these relationships, we hypothesize that Arth_3905 may function as part of the Arth_3115−3117 alkanesulfonate uptake gene cluster.

Expression of Putative Chromate Resistance Proteins. A chromate resistance determinant (CRD) comprised of eight genes is located on an apparent 96 kb plasmid (Arth_4255-Arth_4247) within the FB24 genome. The CRD contains genes encoding chromate efflux proteins (Arth_4248 and Arth_4251), two genes with potential regulatory functions (Arth_4254 and Arth_4253), a malate/quinone oxidoreductase (Arth_4255), a lipoprotein (Arth_4247), and a protein of unknown function (Arth_4252). Each of these genes exhibited induction with increasing concentrations of chromate at the transcript level (K. L. Henne, manuscript submitted). When the cells were grown in lead, hydrogen peroxide and arsenate, there was little or no induction, suggesting a chromate-specific response for this gene set.

The relative expression levels for the corresponding CRD proteins are listed in Table 4. Very high (>20-fold) fold differences were observed for Arth_4247, 4252, 4255 and 4256. The highest observed change [85-fold increase in 5 mM Cr(VI), global partition] was for Arth_4247, annotated as a conserved lipoprotein, similar to the LppY/LpqO group in *Mycobacteria*.[54] Lipoproteins are known to play roles in responding to divalent metals such as copper and lead,[55,56] but the involvement in the response to anionic metal compounds has not been

Table 3. Proteins with Increased Abundance in Cr(VI) from Heat Map Clusters

locus	gene description	relative fold difference (experimental/control)[a] 5 mM Cr(VI)	20 mM Cr(VI)	no Cr(VI) stat
	Replication, Recombination and Repair			
Arth_0672	ATP-dependent DNA helicase, RecQ family	8.7 I	15.3 I	1.7 I
Arth_1211	hydrolase, TatD family	2.0 S	4.7 S	2.0 S
Arth_1520	NUDIX hydrolase	3.0 S	6.0 S	1.0 S
Arth_1581	DNA polymerase III, alpha subunit	4.6 I	5.0 I	1.3 I
Arth_2063	DNA polymerase I	3.2 I	3.6 I	1.5 I
Arth_2074	DEAD/DEAH box helicase domain protein	4.0 G	10.0 G	2.5 S
Arth_2318	DNA polymerase III, alpha subunit	13.0 I	7.0 I	1.0 I
Arth_2756	UvrD/REP helicase	21.0 I	21.0 I	6.0 I
Arth_2757	UvrD/REP helicase	7.0 I	20.0 I	4.0 I
Arth_3798	SNF2-related protein	6.0 I	9.0 I	0.8 G
	Iron Sequestration/DNA protection			
Arth_0334	Ferritin, Dps family protein	6.0 G	4.5 G	2.0 G
Arth_0761	Ferritin, Dps family protein	2.5 S	2.7 S	2.1 S
	General Function Prediction			
Arth_3714	Rieske (2Fe−2S) domain protein	13.0 G	18.0 G	2.0 G
Arth_4252	40-residue YVTN family beta-propeller repeat protein	42.0 G	9.0 G	0.7 G
Arth_4255	malate−quinone oxidoreductase	42.0 I	44.0 S	2.7 I
Arth_4256	aminoglycoside phosphotransferase	25.0 I	30.0 I	1.5 S
	Energy Production and Conversion			
Arth_0129	nitroreductase	13.0 G	5.2 G	0.7 I
Arth_3948	aldo/keto reductase	12.0 G	10.3 G	NO
	Inorganic Ion Transport/Putative Sulfonate Uptake Proteins			
Arth_0806	ABC transporter related	7.0 I	7.0 I	3.0 I
Arth_0857	ABC transporter related	4.0 S	9.0 S	3.0 G
Arth_0858	ABC transporter related	4.5 G	5.0 S	1.3 G
Arth_3115	binding-protein-dependent transport systems inner membrane component	10 I	5 I	NO
Arth_3116	ABC transporter related	15.0 I	7.3 I	0.7 I
Arth_3117	NLPA lipoprotein	21.1 I	13.4 I	1.3 I
Arth_3122	sulfate adenylyltransferase, large subunit	4.6 I	2.8 I	0.5 I
Arth_3123	sulfate adenylyltransferase, small subunit	2.9 G	3.3 S	0.7 S
Arth_3124	phosphoadenosine phosphosulfate reductase	2.3 G	2.0 I	0.7 G
Arth_3125	Ferredoxin--nitrite reductase	2.6 G	2.2 S	1.2 S
Arth_3905	FMNH2-utilizing oxygenase	108 G	58 G	NO

[a] Values reported reflect the highest expression level and the corresponding partition. G = global partition, S = soluble partition, I = Insoluble partition, NO = Not observed.

demonstrated. In the case of copper, the lipoprotein NlpE was shown to stimulate the CpxAR envelope stress responsive pathway in *E. coli*.[56] This signal transduction pathway responds to external stimuli and the role of NlpE in its activation has been established.[56,57] Recently, *E. coli* protein YihE, which has similarities to aminoglycoside phosphotransferase, was determined to be part of a Ser/Thr protein kinase phosphorelay induced by the Cpx stress response.[58] Since Arth_4256 is a putative aminoglycoside phosphotransferase with a Ser/Thr kinase domain, it is possible that a signal transduction cascade is integral to chromate resistance in *Arthrobacter* sp. strain FB24.[59] This is further supported by the increased expression of Arth_4252 under Cr(VI) stress. Arth_4252 is a protein of unknown function that contains a WD40 repeat domain, which is found in a family of structurally similar but functionally diverse proteins. These proteins are thought to perform a wide array of functions in eukaryotes and prokaryotes, but the regulation of responses to environmental stimuli appears to be common. In particular, many WD40 repeat domain proteins participate in detecting cell envelope stress and initiating signal transduction pathways.[60,61]

The function of Arth_4255 is unclear, but its high expression under Cr(VI) stress is indicative of a potential role for Cr(VI) resistance in strain FB24. Arth_4255 encodes a putative malate/quinone oxidoreductase. In other systems, malate/quinone oxidoreductases convert malate to oxaloacetate, with subsequent transfer of electrons to the quinone pool and can operate in both the TCA cycle and in electron transport.[62,63] Reduction of chromate has been demonstrated with other NAD(P)H-dependent quinone oxidoreductases such as YieF from *E. coli* and ChrR from *Pseudomonas putida*[64,65] However, given that these proteins share no sequence similarity to Arth_4255 and that FB24 has not exhibited chromate reduction, it is unlikely that Arth_4255 serves an analogous function to YieF and ChrR.

Of the remaining predicted proteins from the chromate resistance determinant of *Arthrobacter* sp. strain FB24, only Arth_4253 (ChrB-Nterm), a predicted chromate resistance signal protein, was observed in the final peptide data set, exhibiting a 2-fold increase in abundance in the 20 mM Cr(VI) global partition. The absence of the remaining proteins from this genetic region in the proteome data set does not necessarily reflect a lack of expression of Arth_4254 (ChrB-Cterm, chromate resistance related protein), Arth_4248 (ChrA, chromate efflux protein), or Arth_4251 (predicted ORF carrying ChrA conserved domain), but rather is a consequence of the technical difficulties in detecting and quantifying these proteins which

Table 4. Expression of CRD Proteins and Proteins with Similar Expression Profiles

locus	gene description	relative fold difference (experimental/control)[a] 5 mM Cr(VI)	20 mM Cr(VI)	no Cr(VI) stat
	Proteins Encoded by Chromate Resistance Determinant			
Arth_4247	protein of unknown function LppY and LpqO	85 G	21.6 I	2 g
Arth_4248	chromate ion transporter (CHR) family	NO	NO	NO
Arth_4251	hypothetical protein/chromate transport domain	NO	NO	NO
Arth_4252	40-residue YVTN family beta-propeller repeat protein	42 G	9 G	0.7 G
Arth_4253	Chromate resistance signal peptide, ChrB-Nterm	NO	2 G	NO
Arth_4254	Chromate resistance protein, ChrB-Cterm	NO	NO	NO
Arth_4255	malate—quinone oxidoreductase	42 I	44 S	2.7 I
	Amino Acid Transport and Metabolism			
Arth_0642	dehydrogenase	3 S	3 S	1 S
Arth_3746	ABC transporter related	9 I	4 I	1 I
Arth_3901	extracellular solute-binding protein, family 3	82 G	42 G	NO
Arth_3977	amino acid permease-associated region	2 G	1 G	NO
	Signal Transduction			
Arth_0657	response regulator receiver protein	7 G	5.5 S	1 G
Arth_1303	response regulator receiver protein	3 S	3 S	1 S
Arth_1376	signal transduction histidine kinase, LytS	5 I	2.7 I	0.7 I
Arth_3901	extracellular solute-binding protein, family 3	82 G	42 G	NO
Arth_4256	aminoglycoside phosphotransferase	25 I	30 I	1.5 S
	Energy Production and Conversion			
Arth_1300	putative nitrilotriacetate monooxygenase	50 S	35 S	1 S
Arth_1530	sodium:dicarboxylate symporter	52 I	4 I	1 I
Arth_2628	oxidoreductase FAD/NAD(P)-binding domain protein	4.5 I	2.5 I	1.5 I
Arth_3905	FMNH2-utilizing oxygenase	108 G	58 H	NO
	Proteins with No COG Function Assigned			
Arth_0044	hypothetical protein	5 S	4 S	1 S
Arth_0514	hypothetical protein	3 I	2 I	1 I
Arth_2155	hypothetical protein	3 S	NO	1 I
Arth_3867	hypothetical protein	3 I	2 I	NO

[a] Values reported reflect the highest expression level and the corresponding partition. G = global partition, S = soluble partition, I = Insoluble partition, NO = Not observed.

either have low MW or have many membrane-spanning regions. Peptides for each of these proteins were observed in the raw data set, but failed to pass the stringent filtering criteria applied to the raw peptide data.

Proteins with Similar Expression Profiles to the CRD. The LC/LC-MS/MS data were queried to search for proteins exhibiting similar expression profiles to those from the genetically characterized CRD (Table 4). There were 23 proteins with at least a 2-fold increase in at least one partition under Cr(VI) conditions. The major COG functional categories represented by this group are amino acid transport and metabolism, signal transduction mechanisms, and energy production and conversion. Five of the 23 proteins were not associated with any of the COG functional categories. These included 4 hypothetical proteins and one protein with a CBS (cystathionine beta-synthase) domain (Arth_2644).

Expression of Arth_3901 increased 82-fold and 42-fold in the global partition for 5 and 20 mM Cr(VI), respectively. On the basis of sequence similarity, Arth_3901 falls within extracellular solute-binding class 3 family of proteins (CDD search $E = 5 \times 10^{-21}$), which is specific for polar amino acids and opines.[66] Polar amino acids consist of the basic and acidic amino acids (Lys, Arg, His, Asp, Glu), in addition to polar, uncharged amino acids (Ser, Thr, Pro, Asn, Gln). Cysteine is often considered as part of this latter group and increased expression of Arth_3901 in Cr(VI)-exposed cells may reflect an attempt to take up alternative sulfur sources. Further support is provided by the sequence similarity of Arth_3901 to potential cysteine and cystine uptake proteins (*Klebsiella pneumonia* cysteine transport protein $E = 8 \times 10^{-80}$, 52% aa identity and *E. coli* cystine-binding periplasmic protein precursor $E = 7 \times 10^{-14}$, 27% aa identity) and the presence of a PBPb conserved domain (CDD search $E = 1 \times 10^{-14}$), which is found in transport proteins specific for a wide variety of substrates including amino acids and inorganic anions such as sulfate.[67] Of further interest for its potential role in the uptake of aliphatic sulfonates is Arth_1300, which exhibited a 50 and 35-fold increase in the soluble partition for 5 and 20 mM Cr(VI), respectively. Like the protein clusters listed in Table 3, it is suspected that this protein is also part of a Cr(VI)-induced sulfate limitation response.

Proteins Involved in Carbohydrate Metabolism, Energy Production, and Amino Acid Transport and Metabolism. After assigning COG functions to the proteins with at least a 2-fold change in the experimental conditions versus the 0 mM Cr(VI) log-phase control, the majority of proteins showing altered expression in each partition occurred in the categories of carbohydrate transport and metabolism, energy production and conversion, and amino acid transport and metabolism. However, the functional roles of a given protein may overlap categories. For instance, some enzymes involved in carbohydrate transport and metabolism may also be integral to energy production and conversion. In the same manner, key reactions where metabolic pathways merge, such as glycolysis and the TCA cycle, serve as entry points into amino acid metabolism and other anaplerotic pathways. With this in mind, a pathway approach was taken to identify proteins within COG categories

Table 5. Proteins Involved in Carbohydrate Metabolism and Energy Production and Conversion

locus	gene description	relative fold difference (experimental/control)[a] 5 mM Cr(VI)	20 mM Cr(VI)	no Cr(VI) stat
	Glycolysis and Gluconeogenesis			
Arth_0518	fructose-bisphosphate aldolase, class II	0.5 I	0.6 I	0.8 I
Arth_1147	Phosphopyruvate hydratase	0.8 I	0.5 I	0.8 I
Arth_1693	Pyruvate kinase	0.5 I	0.7 I	0.6 I
Arth_2438	glyceraldehyde-3-phosphate dehydrogenase	0.6 I	0.3 G	0.7 I
Arth_3003	6-phosphofructokinase	2.4 G	0.2 I	0.2 I
	Pyruvate Metabolism			
Arth_0614	Phosphoenolpyruvate carboxylase	3.5 I	2.0 I	2.0 I
Arth_0667	Phosphoenolpyruvate carboxykinase (GTP)	0.7 I	0.2 I	0.3 I
Arth_1160	acetyl-CoA acetyltransferases	1.2 G	0.4 G	1.4 I
Arth_1381	Pyruvate dehydrogenase (acetyl-transferring)	2.0 I	0.3 I	2.0 I
Arth_1856	Aldehyde dehydrogenase (NAD(+))	0.5 G	0.5 G	3.5 G
Arth_1972	phosphoenolpyruvate synthase	0.2 I	0.1 I	0.4 I
Arth_2549	malate--quinone oxidoreductase	2.2 I	1.3 I	1.4 I
Arth_2564	Pyruvate dehydrogenase (acetyl-transferring)	0.6 G	0.2 G	1.4 G
Arth_2986	acetyl-CoA acetyltransferases	0.5 G	0.4 G	1.8 S
Arth_3088	Aldehyde dehydrogenase (NAD(+))	0.2 I	0.1 I	0.3 I
Arth_3193	Pyruvate dehydrogenase (acetyl-transferring)	0.9 G	0.3 G	0.3 G
Arth_3240	phosphate acetyltransferase	3.1 S	1.7 S	3.0 I
Arth_3268	acetyl-CoA acetyltransferases	0.2 I	0.3 I	1.3 G
Arth_3343	L-lactate dehydrogenase (cytochrome)	1.9 I	0.3 I	0.7 S
Arth_3432	Malate dehydrogenase (oxaloacetate-decarboxylating)	0.5 I	0.3 G	0.4 I
Arth_3994	Malate dehydrogenase (oxaloacetate-decarboxylating)	0.3 I	0.2 I	0.3 S
Arth_4073	acetyl-CoA acetyltransferases	0.6 G	0.2 G	0.4 G
	Pentose-Phosphate Pathway and TCA Cycle			
Arth_0143	Fructose-6-phosphate phosphoketolase	0.3 I	0.3 I	2.1 G
Arth_0518	Fructose-bisphosphate aldolase	0.5 I	0.6 I	0.8 I
Arth_0815	Succinyl-CoA synthetase, beta subunit	1.6 S	0.5 I	0.5 I
Arth_1092	Isocitrate dehydrogenase, NADP-dependent	0.7 I	0.6 I	0.5 I
Arth_1129	Succinate dehydrogenase, flavoprotein subunit	2.0 I	2.0 S	1.4 I
Arth_1523	2-methylcitrate synthase/citrate synthase II	0.6 I	0.1 I	1.5 I
Arth_2490	Glucose-6-phospate 1-dehydrogenase	0.4 G	0.6 G	1.5 S

[a] Greatest fold-difference (up or down) observed in the designated partition for proteins exhibiting at least a 2-fold change in either Cr(VI) condition. G = global partition, S = soluble partition, I = insoluble partition.

whose altered expression may play a pivotal role in the cellular response to chromate stress.

One hundred and forty proteins were observed across all partitions in the carbohydrate transport and metabolism category and 112 proteins were observed in the energy production and conversion category. Proteins involved in glycolysis, the pentose-phosphate pathway and TCA cycle were examined for differential expression under chromate stress (Table 5). The link between glycolysis and the TCA cycle centers on pyruvate metabolism. The reactions that define this node include the interconversion of phosphoenolpyruvate (PEP), pyruvate and oxaloacetate, which ultimately direct the carbon flux through central metabolism and anaplerosis.[68] Twenty-three proteins involved in pyruvate metabolism exhibited a 2-fold or greater difference in expression under Cr(VI) stress. This includes decreased abundance of a number of enzymes involved in the production of PEP and pyruvate and the slight increase in abundance of pyruvate carboxylase (Arth_0614). Components of the pyruvate dehydrogenase complex and aldehyde dehydrogenase also exhibited lower abundance under Cr(VI) stress, which could lead to decreased flux toward acetyl-CoA and subsequently, a decrease in fueling of the TCA cycle. These collective findings would have negative effects on the synthesis of amino acids, nucleic acids, lipids and overall energy production,[68] which is consistent with the growth defects exhibited by *Arthrobacter* sp. strain FB24 above 5 mM Cr(VI).

One hundred and seventy-six proteins involved in amino acid transport and metabolism showed altered expression profiles in Cr(VI) conditions (Table 6). Protein clusters with putative functions in leucine, isoleucine and valine transport (Arth_1154−1156), glutamate uptake (Arth_2801−2804), serine/glycine transport and metabolism (Arth_3700−3705) and histidine biosynthesis (Arth_0969−0972) all show decreased abundance under Cr(VI) stress. Conversely, a number of proteins within the cysteine metabolic pathway have fold differences of at least 2 or higher under Cr(VI) stress. Arth_2446 (cysteine synthase) and Arth_2447 (serine *O*-acetyltransferase), which function in the assimilation of sulfur to produce cysteine,[69] were increased 2- to 4-fold in the Cr(VI) conditions across each partition. Likewise, proteins comprising the sulfur assimilation pathway through the action of sulfate adenylyltransferase and PAPS reductase[70] (Arth_3122−3124) were expressed in a similar fashion. These results are similar to those seen for *E. coli*[43] and *S. oneidensis*[44] when each strain was subjected to chromate stress.

Conclusions

In this study, the global proteomic response of *Arthrobacter* sp. strain FB24 to chromate was examined. Although strain FB24 can tolerate Cr(VI) up to 200 mM, a decrease in growth rate and biomass yield is observed at Cr(VI) concentrations of

Table 6. Proteins Involved in Amino Acid Uptake and Metabolism

locus	gene description	greatest relative fold difference (experimental/control)[a] 5 mM Cr(VI)	20 mM Cr(VI)	no Cr(VI) stat
	Isoleucine, Leucine and Valine Metabolism			
Arth_1154	Extracellular ligand receptor	1.7 I	0.3 I	1.9 I
Arth_1155	ABC transporter related	1.7 I	0.1 I	3.1 I
Arth_1156	ABC transporter related	0.2 S	0.3 S	0.5 S
	Glutamate Uptake			
Arth_2801	ABC transporter related	1.7 I	0.5 G	2.3 I
Arth_2802	Extracellular solute-binding protein, family 3	1.7 I	0.4 I	2.0 S
Arth_2804	Polar amino acid ABC transporter, inner membrane component	0.5 G	0.7 I	3.7 I
Arth_2805	Succinyl-diaminopimelate desuccinlyase	7.0 I	2.0 I	4.0 I
	Serine/Glycine Metabolism			
Arth_3700	L-serine dehydratase 1	0.3 S	0.2 S	0.8 S
Arth_3701	Sarcosine oxidase, gamma subunit	0.3 I	0.2 G	0.4 G
Arth_3702	Sarcosine oxidase, alpha subunit	0.3 I	0.3 I	0.6 I
Arth_3703	Sarcosine oxidase, delta subunit	0.3 G	0.1 G	0.6 G
Arth_3704	Sarcosine oxidase, beta subunit family	0.3 I	0.2 I	0.4 I
Arth_3705	Glycine hydroxymethyltransferase	0.5 I	0.2 G	0.5 G
	Histidine Metabolism			
Arth_0969	Thiamine pyrophosphate enzyme TPP binding domain	0.2 I	0.1 I	0.1 I
Arth_0971	Histidinol-phosphate aminotransferase	0.1 G	0.1 G	0.2 S
Arth_0972	Amino acid permease-associated region	0.2 G	NO	0.2 G
	Cysteine Synthesis			
Arth_2446	Cysteine synthase A	4.3 I	3.5 S	1.2 S
Arth_2447	Serine *O*-acetyltransferase	2.8 G	3.0 G	1.5 G
Arth_3122	sulfate adenylyltransferase subunit 1	4.6 I	2.8 I	0.3 G
Arth_3123	Sulfate adenylyltransferase small subunit	2.9 G	3.3 S	0.2 G
Arth_3124	Phosphoadenosine phosphosulfate reductase	2.3 G	2.0 I	0.2 S

[a] Greatest fold-difference (up or down) observed in the designated partition for proteins exhibiting at least a 2-fold change in either Cr(VI) condition. G = global partition, S = soluble partition, I = insoluble partition, NO = not observed.

5 mM or greater. The objective here was to identify proteins whose expression changes in response to Cr(VI) exposure and those that play a role in Cr(VI) resistance. The greatest proportion of differentially expressed proteins included those involved in carbohydrate metabolism, amino acid metabolism, and energy production and conversion. Thirty-two percent (140 proteins) of the 436 FB24 proteins predicted to function in carbohydrate transport and metabolism, 46% (167 proteins) of the 364 proteins involved in amino acid transport and metabolism, and 47% (112 proteins) of the 239 proteins that fall within the energy production and conversion category exhibited at least a 2-fold change in abundance under chromate stress.

A large number of these proteins are active at the pyruvate node, a major hub of central primary metabolism, joining carbohydrate metabolism, energy production and amino acid biosynthesis. However, the proteins exhibiting the highest fold increases in response to Cr(VI) stress were ones expected to be expressed when cell growth was limited by sulfur. At least 16 proteins with potential roles in the uptake of alternative sulfur sources and cysteine synthesis exhibited elevated expression. Chromate toxicity is further marked by oxidative damage to macromolecules,[43] and the role of cysteine in potentially minimizing cellular oxidative damage should not be overlooked.[71,72]

The expression of proteins encoded by genes within the plasmid-borne CRD of strain FB24 was also observed, confirming what was observed at the transcript level. Arth_4256, an aminoglycoside phosphotransferase directly downstream of Arth_4255, was also expressed at higher levels in response to Cr(VI) and is a potential target for further studies at the genetic level to determine if it is essential to Cr(VI) resistance in this strain. Considering the potential roles of these proteins in signal transduction and environmental stress response, along with the putative regulatory roles of Arth_4253 and 4254, ChrB-Nterm and ChrB-Cterm, respectively, we expect that chromate efflux in strain FB24 is regulated by a signal transduction pathway. Moreover, the increased abundance of proteins within the CRD that have not been shown previously to function in Cr(VI) resistance in other bacteria could further explain the high Cr(VI) resistance of FB24 compared to other, well-studied organisms.

Abbreviations: CRD, Chromate Resistance Determinant; CHR, chromate ion transporter; Cr(VI), chromate; COG, Clusters of Orthologous Groups.

Acknowledgment. K. L. Henne thanks Angela Ahrendt, Tripti Khare and Jessica Smotrys of Argonne National Laboratory for thoughtful discussion and laboratory assistance and the W.M. Keck Foundation Biotechnology Resource Laboratory for assistance with protein identification. This work was supported by a grant from the Department of Energy's Environmental Remediation Science Program (grant DE-FG02-98ER62681). K.H. received support from the Purdue Research Foundation and the Purdue Graduate School Bilsland Doctoral Fellowship. The research described in this paper was conducted in part under the Laboratory Directed Research and Development Program at Pacific Northwest National Laboratory, a multiprogram national laboratory operated by Battelle for the U.S. Department of Energy under Contract DE-AC05-76RL01830. A portion of the research described in this paper was performed in the

Environmental Molecular Sciences Laboratory, a national scientific user facility sponsored by the Department of Energy's Office of Biological and Environmental Research and located at Pacific Northwest National Laboratory. Portions of the proteomics work were supported under the Proteomic Biological Applications Project by the Genomics: GTL program in the Department of Energy Office of Biological and Environmental Research. The work done at Argonne National Laboratory, a U.S. Department of Energy Office of Science laboratory operated by UChicago Argonne, LLC, was funded through Contract No. DE-AC02-06CH11357 as part of the Microbial Proteome Project of the DOE OBER Genomics GtL Program.

Supporting Information Available: Supplemental Tables 1−3 contain the complete list and peptide abundance values of proteins with at least a 2-fold change in abundance identified from the LC/LC-MS/MS method. Supplemental Table 4 contains the list of proteins identified from the 2-DGE method and the corresponding peptide abundance values observed with LC/LC-MS/MS. Supplemental Table 5 contains p*I* and MW data for proteins identified by 2-DGE. Growth curves of strain FB24 in 0, 5, and 20 mM Cr(VI) are provided in Supplemental Figure 1. This material is available free of charge via the Internet at http://pubs.acs.org.

References

(1) Jones, D.; Keddie, R. M. The Genus Arthrobacter. In *The Prokaryotes: An Evolving Electronic Resource for the Microbiological Community*, 3rd edition, release 3.0 ed.; Dworkin, M., Ed. Springer-Verlag: New York, 1999.

(2) Benyehuda, G.; Coombs, J.; Ward, P. L.; Balkwill, D.; Barkay, T. Metal resistance among aerobic chemoheterotrophic bacteria from the deep terrestrial subsurface. *Can. J. Microbiol.* **2003**, *49* (2), 151–156.

(3) Crocker, F. H.; Fredrickson, J. K.; White, D. C.; Ringelberg, D. B.; Balkwill, D. L. Phylogenetic and physiological diversity of Arthrobacter strains isolated from unconsolidated subsurface sediments. *Microbiology* **2000**, *146* (6), 1295–1310.

(4) Fredrickson, J. K.; Zachara, J. M.; Balkwill, D. L.; Kennedy, D.; Li, S. M.; Kostandarithes, H. M.; Daly, M. J.; Romine, M. F.; Brockman, F. J. Geomicrobiology of high-level nuclear waste-contaminated vadose sediments at the Hanford site, Washington state. *Appl. Environ. Microbiol.* **2004**, *70* (7), 4230–4241.

(5) Garten, C. T., Jr.; Hamby, D. M.; Schreckhise, R. G. Radiocesium discharges and subsequent environmental transport at the major US weapons production facilities. *Sci. Total Environ.* **2000**, *255* (1−3), 55–73.

(6) Kimbrough, D. E.; Cohen, Y.; Winer, A. M.; Creelman, L.; Mabuni, C. A critical assessment of chromium in the environment. *Crit. Rev. Environ. Sci. Technol.* **1999**, *29* (1), 1–46.

(7) Ding, M.; Shi, X. Molecular mechanisms of Cr(VI)-induced carcinogenesis. *Mol. Cell. Biochem.* **2002**, *234−235* (1−2), 293–300.

(8) Giller, K. E.; Witter, E.; McGrath, S. P. Toxicity of heavy metals to microorganisms and microbial processes in agricultural soils: A review. *Soil Biol. Biochem.* **1998**, *30* (10−11), 1389–1414.

(9) Nakatsu, C. H.; Carmosini, N.; Baldwin, B.; Beasley, F.; Kourtev, P.; Konopka, A. Soil microbial community responses to additions of organic carbon substrates and heavy metals (Pb and Cr). *Appl. Environ. Microbiol.* **2005**, *71* (12), 7679–89.

(10) Beasley, F. C. Characterization of Diversity, Chromate Resistance and Aromatic Hydrocarbon Degradation Among Arthrobacter Isolates from Mixed Waste Soil. Masters Thesis, Purdue University, West Lafayette, IN 2004.

(11) Camargo, F. A.; Okeke, B. C.; Bento, F. M.; Frankenberger, W. T. Diversity of chromium-resistant bacteria isolated from soils contaminated with dichromate. *Appl. Soil Ecol.* **2005**, *29*, 193–202.

(12) Cervantes, C.; Silver, S. Plasmid chromate resistance and chromate reduction. *Plasmid* **1992**, *27* (1), 65–71.

(13) Juhnke, S.; Peitzsch, N.; Hubener, N.; Grosse, C.; Nies, D. H. New genes involved in chromate resistance in *Ralstonia metallidurans* strain CH34. *Arch. Microbiol.* **2002**, *179* (1), 15–25.

(14) Viti, C.; Pace, A.; Giovannetti, L. Characterization of Cr(VI)-resistant bacteria isolated from chromium-contaminated soil by tannery activity. *Curr. Microbiol.* **2003**, *46* (1), 1–5.

(15) Viti, C.; Decorosi, F.; Tatti, E.; Giovannetti, L. Characterization of chromate-resistant and -reducing bacteria by traditional means and by a high-throughput phenomic technique for bioremediation purposes. *Biotechnol. Prog.* **2007**, *23* (3), 553–559.

(16) Giometti, C. S.; Reich, C.; Tollaksen, S.; Babnigg, G.; Lim, H.; Zhu, W.; Yates, J.; Olsen, G. Global analysis of a "simple" proteome: *Methanococcus jannaschii*. *J. Chromatogr., B: Anal. Technol. Biomed. Life Sci.* **2002**, *782* (1−2), 227–243.

(17) VanBogelen, R. A.; Schiller, E. E.; Thomas, J. D.; Neidhardt, F. C. Diagnosis of cellular states of microbial organisms using proteomics. *Electrophoresis* **1999**, *20* (11), 2149–2159.

(18) Evans, C. R.; Jorgenson, J. W. Multidimensional LC-LC and LC-CE for high-resolution separations of biological molecules. *Anal. Bioanal. Chem.* **2004**, *378* (8), 1952–1961.

(19) Norbeck, A. D.; Callister, S. J.; Monroe, M. E.; Jaitly, N.; Elias, D. A.; Lipton, M. S.; Smith, R. D. Proteomic approaches to bacterial differentiation. *J. Microbiol. Methods* **2006**, *67* (3), 473–486.

(20) Ramagli, L. S. Quantifying protein in 2-D PAGE solubilization buffers. *Methods Mol. Biol.* **1999**, *112*, 99–103.

(21) Anderson, N. G.; Anderson, N. L. Analytical techniques for cell fractions. XXI. Two-dimensional analysis of serum and tissue proteins: multiple isoelectric focusing. *Anal. Biochem.* **1978**, *85* (2), 331–340.

(22) Anderson, N. L.; Anderson, N. G. Analytical techniques for cell fractions. XXII. Two-dimensional analysis of serum and tissue proteins: multiple gradient-slab gel electrophoresis. *Anal. Biochem.* **1978**, *85* (2), 341–354.

(23) O'Farrell, P. H. High resolution two-dimensional electrophoresis of proteins. *J. Biol. Chem.* **1975**, *250* (10), 4007–4021.

(24) Giometti, C. S.; Gemmell, M. A.; Tollaksen, S. L.; Taylor, J. Quantitation of human leukocyte proteins after silver staining: a study with two-dimensional electrophoresis. *Electrophoresis* **1991**, *12* (7−8), 536–543.

(25) Giometti, C. S.; Tollaksen, S. L.; Gemmell, M. A.; Burcham, J.; Peraino, C. A heritable variant of mouse liver ornithine aminotransferase (EC 2.6.1.13) induced by ethylnitrosourea. *J. Biol. Chem.* **1988**, *263* (30), 15781–15784.

(26) Ahrendt, A. J.; Tollaksen, S. L.; Lindberg, C.; Zhu, W.; Yates, J. R., III; Nevin, K. P.; Babnigg, G.; Lovley, D. R.; Giometti, C. S. Steady state protein levels in Geobacter metallireducens grown with iron (III) citrate or nitrate as terminal electron acceptor. *Proteomics* **2007**, *7* (22), 4148–4157.

(27) Lipton, M. S.; Pasa-Tolic, L.; Anderson, G. A.; Anderson, D. J.; Auberry, D. L.; Battista, J. R.; Daly, M. J.; Fredrickson, J.; Hixson, K. K.; Kostandarithes, H.; Masselon, C.; Markillie, L. M.; Moore, R. J.; Romine, M. F.; Shen, Y.; Stritmatter, E.; Tolic, N.; Udseth, H. R.; Venkateswaran, A.; Wong, K.-K.; Zhao, R.; Smith, R. D. From the Cover: Global analysis of the Deinococcus radiodurans proteome by using accurate mass tags. *Proc. Natl. Acad. Sci. U.S.A.* **2002**, *99* (17), 11049–11054.

(28) Smith, R. D.; Anderson, G. A.; Lipton, M. S.; Pasa-Tolic, L.; Shen, Y.; Conrads, T. P.; Veenstra, T. D.; Udseth, H. R. An accurate mass tag strategy for quantitative and high-throughput proteome measurements. *Proteomics* **2002**, *2* (5), 513–523.

(29) Lipton, M. S.; Romine, M. F.; Monroe, M. E.; Elias, D. A.; Pasa-Tolic, L.; Anderson, G. A.; Anderson, D. J.; Fredrickson, J.; Hixson, K. K.; Masselon, C.; Mottaz, H.; Tolic, N.; Smith, R. D. AMT tag approach to proteomic characterization of Deinococcus radiodurans and Shewanella oneidensis. *Methods Biochem. Anal.* **2006**, *49*, 113–134.

(30) Eng, J. K.; McCormack, A. L.; Yates, J. R., III. An approach to correlate tandem mass spectral data of peptides with amino acid sequences in a protein database. *J. Am. Soc. Mass Spectrom.* **1994**, *5* (11), 976–989.

(31) Washburn, M. P.; Wolters, D.; Yates, J. R., III. Large-scale analysis of the yeast proteome by multidimensional protein identification technology. *Nat. Biotechnol.* **2001**, *19* (3), 242–247.

(32) Qian, W. J.; Liu, T.; Monroe, M. E.; Strittmatter, E. F.; Jacobs, J. M.; Kangas, L. J.; Petritis, K.; Camp, D. G., II; Smith, R. D. Probability-based evaluation of peptide and protein identifications from tandem mass spectrometry and SEQUEST analysis: the human proteome. *J. Proteome Res.* **2005**, *4* (1), 53–62.

(33) Lu, P.; Vogel, C.; Wang, R.; Yao, X.; Marcotte, E. M. Absolute protein expression profiling estimates the relative contributions of transcriptional and translational regulation. *Nat. Biotechnol.* **2007**, *25* (1), 117–124.

(34) Wang, H.; Qian, W. J.; Chin, M. H.; Petyuk, V. A.; Barry, R. C.; Liu, T.; Gritsenko, M. A.; Mottaz, H. M.; Moore, R. J.; Camp Ii, D. G.;

Khan, A. H.; Smith, D. J.; Smith, R. D. Characterization of the mouse brain proteome using global proteomic analysis complemented with cysteinyl-peptide enrichment. *J. Proteome Res.* **2006**, *5* (2), 361–369.
(35) Zhu, W.; Reich, C. I.; Olsen, G. J.; Giometti, C. S.; Yates, J. R., III. Shotgun proteomics of *Methanococcus jannaschii* and insights into methanogenesis. *J. Proteome Res.* **2004**, *3* (3), 538–548.
(36) Ziegler, D. M. Role of reversible oxidation-reduction of enzyme thiols-disulfides in metabolic regulation. *Annu. Rev. Biochem.* **1985**, *54*, 305–329.
(37) Moran, L. K.; Gutteridge, J. M.; Quinlan, G. J. Thiols in cellular redox signalling and control. *Curr. Med. Chem.* **2001**, *8* (7), 763–772.
(38) Fucci, L.; Oliver, C. N.; Coon, M. J.; Stadtman, E. R. Inactivation of key metabolic enzymes by mixed-function oxidation reactions: possible implication in protein turnover and ageing. *Proc. Natl. Acad. Sci. U.S.A.* **1983**, *80* (6), 1521–1525.
(39) Tamarit, J.; Cabiscol, E.; Ros, J. Identification of the major oxidatively damaged proteins in *Escherichia coli* cells exposed to oxidative stress. *J. Biol. Chem.* **1998**, *273* (5), 3027–3032.
(40) Weber, H.; Engelmann, S.; Becher, D.; Hecker, M. Oxidative stress triggers thiol oxidation in the glyceraldehyde-3-phosphate dehydrogenase of *Staphylococcus aureus*. *Mol. Microbiol.* **2004**, *52* (1), 133–140.
(41) Kamada, N.; Yasuhara, A.; Takano, Y.; Nakano, T.; Ikeda, M. Effect of transketolase modifications on carbon flow to the purine-nucleotide pathway in *Corynebacterium ammoniagenes*. *Appl. Microbiol. Biotechnol.* **2001**, *56* (5−6), 710–717.
(42) Ohtake, H.; Cervantes, C.; Silver, S. Decreased chromate uptake in *Pseudomonas fluorescens* carrying a chromate resistance plasmid. *J. Bacteriol.* **1987**, *169* (8), 3853–3856.
(43) Ackerley, D. F.; Barak, Y.; Lynch, S. V.; Curtin, J.; Matin, A. Effect of chromate stress on *Escherichia coli* K-12. *J. Bacteriol.* **2006**, *188* (9), 3371–3381.
(44) Brown, S. D.; Thompson, M. R.; Verberkmoes, N. C.; Chourey, K.; Shah, M.; Zhou, J.; Hettich, R. L.; Thompson, D. K. Molecular dynamics of the *Shewanella oneidensis* response to chromate stress. *Mol. Cell. Proteomics* **2006**, *5* (6), 1054–1071.
(45) Hu, P.; Brodie, E. L.; Suzuki, Y.; McAdams, H. H.; Andersen, G. L. Whole-genome transcriptional analysis of heavy metal stresses in *Caulobacter crescentus*. *J. Bacteriol.* **2005**, *187* (24), 8437–8449.
(46) Thompson, M. R.; Verberkmoes, N. C.; Chourey, K.; Shah, M.; Thompson, D. K.; Hettich, R. L. Dosage-dependent proteome response of *Shewanella oneidensis* MR-1 to acute chromate challenge. *J. Proteome Res.* **2007**, *6* (5), 1745–1757.
(47) Lipton, M. S.; Pasa-Tolic, L.; Anderson, G. A.; Anderson, D. J.; Auberry, D. L.; Battista, J. R.; Daly, M. J.; Fredrickson, J.; Hixson, K. K.; Kostandarithes, H.; Masselon, C.; Markillie, L. M.; Moore, R. J.; Romine, M. F.; Shen, Y.; Stritmatter, E.; Tolic, N.; Udseth, H. R.; Venkateswaran, A.; Wong, K.-K.; Zhao, R.; Smith, R. D. From the Cover: Global analysis of the *Deinococcus radiodurans* proteome by using accurate mass tags. *Proc. Natl. Acad. Sci. U.S.A.* **2002**, *99* (17), 11049–11054.
(48) Carrondo, M. A. Ferritins, iron uptake and storage from the bacterioferritin viewpoint. *EMBO J.* **2003**, *22* (9), 1959–1968.
(49) Miranda, A. T.; Gonzalez, M. V.; Gonzalez, G.; Vargas, E.; Campos-Garcia, J.; Cervantes, C. Involvement of DNA helicases in chromate resistance by *Pseudomonas aeruginosa* PAO1. *Mutat. Res.* **2005**, *578* (1−2), 202–209.
(50) Wang, C. C.; Newton, A. Iron transport in *Escherichia coli*: relationship between chromium sensitivity and high iron requirement in mutants of *Escherichia coli*. *J. Bacteriol.* **1969**, *98* (3), 1135–1141.
(51) Bagchi, D.; Stohs, S. J.; Downs, B. W.; Bagchi, M.; Preuss, H. G. Cytotoxicity and oxidative mechanisms of different forms of chromium. *Toxicology* **2002**, *180* (1), 5–22.
(52) van der Ploeg, J. R.; Cummings, N. J.; Leisinger, T.; ConnertonI. F. Bacillus subtilis genes for the utilization of sulfur from aliphatic sulfonates. *Microbiology* **1998**, *144* (9), 2555–2561.
(53) van Der Ploeg, J. R.; Iwanicka-Nowicka, R.; Bykowski, T.; Hryniewicz, M. M.; Leisinger, T. The Escherichia coli ssuEADCB gene cluster is required for the utilization of sulfur from aliphatic sulfonates and is regulated by the transcriptional activator Cbl. *J. Biol. Chem.* **1999**, *274* (41), 29358–29365.
(54) Sutcliffe, I. C.; Harrington, D. J. Lipoproteins of Mycobacterium tuberculosis: an abundant and functionally diverse class of cell envelope components. *FEMS Microbiol. Rev.* **2004**, *28* (5), 645–659.
(55) Borremans, B.; Hobman, J. L.; Provoost, A.; Brown, N. L.; van Der Lelie, D. Cloning and functional analysis of the pbr lead resistance determinant of Ralstonia metallidurans CH34. *J. Bacteriol.* **2001**, *183* (19), 5651–5658.
(56) Yamamoto, K.; Ishihama, A. Transcriptional response of Escherichia coli to external copper. *Mol. Microbiol.* **2005**, *56* (1), 215–227.
(57) Snyder, W. B.; Davis, L. J.; Danese, P. N.; Cosma, C. L.; Silhavy, T. J. Overproduction of NlpE, a new outer membrane lipoprotein, suppresses the toxicity of periplasmic LacZ by activation of the Cpx signal transduction pathway. *J. Bacteriol.* **1995**, *177* (15), 4216–4223.
(58) Zheng, J.; He, C.; Singh, V. K.; Martin, N. L.; Jia, Z. Crystal structure of a novel prokaryotic Ser/Thr kinase and its implication in the Cpx stress response pathway. *Mol. Microbiol.* **2007**, *63* (5), 1360–1371.
(59) Han, G.; Zhang, C. C. On the origin of Ser/Thr kinases in a prokaryote. *FEMS Microbiol. Lett.* **2001**, *200* (1), 79–84.
(60) Joshi, B.; Janda, L.; Stoytcheva, Z.; Tichy, P. PkwA, a WD-repeat protein, is expressed in spore-derived mycelium of Thermomonospora curvata and phosphorylation of its WD domain could act as a molecular switch. *Microbiology* **2000**, *146* (12), 3259–3267.
(61) Neer, E. J.; Schmidt, C. J.; Nambudripad, R.; Smith, T. F. The ancient regulatory-protein family of WD-repeat proteins. *Nature* **1994**, *371* (6495), 297–300.
(62) Molenaar, D.; van der Rest, M. E.; Drysch, A.; Yucel, R. Functions of the membrane-associated and cytoplasmic malate dehydrogenases in the citric acid cycle of *Corynebacterium glutamicum*. *J. Bacteriol.* **2000**, *182* (24), 6884–6891.
(63) Kather, B.; Stingl, K.; van der Rest, M. E.; Altendorf, K.; Molenaar, D. Another unusual type of citric acid cycle enzyme in *Helicobacter pylori*: the malate:quinone oxidoreductase. *J. Bacteriol.* **2000**, *182* (11), 3204–3209.
(64) Ackerley, D. F.; Gonzalez, C. F.; Park, C. H.; Blake, R., 2nd; Keyhan, M.; Matin, A. Chromate-reducing properties of soluble flavoproteins from *Pseudomonas putida* and *Escherichia coli*. *Appl. Environ. Microbiol.* **2004**, *70* (2), 873–882.
(65) Gonzalez, C. F.; Ackerley, D. F.; Lynch, S. V.; Matin, A. ChrR, a soluble quinone reductase of *Pseudomonas putida* that defends against H_2O_2. *J. Biol. Chem.* **2005**, *280* (24), 22590–22595.
(66) Tam, R.; Saier, M. H. Structural, functional, and dvolutionary relationships among extracellular solute-binding recpetors of bacteria. *Microbiol. Rev.* **1993**, *57* (2), 320–346.
(67) Keskin, O.; Jernigan, R. L.; Bahar, I. Proteins with similar architecture exhibit similar large-scale dynamic behavior. *Biophys. J.* **2000**, *78* (4), 2093–2106.
(68) Sauer, U.; Eikmanns, B. J. The PEP-pyruvate-oxaloacetate node as the switch point for carbon flux distribution in bacteria. *FEMS Microbiol. Rev.* **2005**, *29* (4), 765–794.
(69) Pye, V. E.; Tingey, A. P.; Robson, R. L.; Moody, P. C. The structure and mechanism of serine acetyltransferase from *Escherichia coli*. *J. Biol. Chem.* **2004**, *279* (39), 40729–40736.
(70) Leyh, T. S.; Taylor, J. C.; Markham, G. D. The sulfate activation locus of *Escherichia coli* K12: cloning, genetic, and enzymatic characterization. *J. Biol. Chem.* **1988**, *263* (5), 2409–2416.
(71) Even, S.; Burguiere, P.; Auger, S.; Soutourina, O.; Danchin, A.; Martin-Verstraete, I. Global control of cysteine metabolism by CymR in *Bacillus subtilis*. *J. Bacteriol.* **2006**, *188* (6), 2184–2197.
(72) Lithgow, J. K.; Hayhurst, E. J.; Cohen, G.; Aharonowitz, Y.; Foster, S. J. Role of a cysteine synthase in *Staphylococcus aureus*. *J. Bacteriol.* **2004**, *186* (6), 1579–1590.

PR800705F